ELSEVIER

Thermochimica Acta 399 (2003) 57–62

thermochimica acta

www.elsevier.com/locate/tca

Synthesis and characterization of dibarium iron(II) formate tetrahydrate

Violeta Z. Vassileva*

Institute of General and Inorganic Chemistry, Bulgarian Academy of Sciences, Acad. G. Bonchev Str. Bl. 11, Sofia 1113, Bulgaria

Received 17 April 2002; received in revised form 1 July 2002; accepted 23 July 2002

Abstract

The $Ba(HCOO)_2$–$Fe(HCOO)_2$–H_2O system has been studied by the solubility method at 25 °C and formation of a new double salt with composition $Ba_2Fe(HCOO)_6{\cdot}4H_2O$ was established. The double salt has been characterized by X-ray powder diffraction and thermal analysis. $Ba_2Fe(HCOO)_6{\cdot}4H_2O$ is isostructural with the double salts $Ba_2Me(HCOO)_6{\cdot}4H_2O$ (Me = Co, Ni, Cu, and Zn) and crystallizes in the triclinic system (space group $P\bar{1}$) with lattice parameters $a = 8.902(3)$ Å, $b = 7.125(2)$ Å, $c = 6.901(3)$ Å, $\alpha = 98.85(5)^\circ$, $\beta = 108.81(4)^\circ$, and $\gamma = 82.47(3)^\circ$. The presence of two steps in the thermal dehydration process of the double salt has been established by means of DSC at lower heating rates. The enthalpy of dehydration has been determined.

Keywords: Barium-iron(II) formate double salt; X-ray; DTA; DSC; Heat of dehydration

1. Introduction

It is known that barium formate forms with some metal(II) formates double salts of the type $Ba_2Me(HCOO)_6{\cdot}4H_2O$ (Me = Co, Ni, Cu, and Zn) [1,2]. The double salts are triclinic with space group $P\bar{1}$ and possess nearly identical lattice parameters which means that they are isostructural [3,4]. Only the crystal structure of the copper analogue is reported in the literature [3]. $Ba_2Cu(HCOO)_6{\cdot}4H_2O$ crystallizes in the triclinic system with space group $P\bar{1}$ and with lattice parameters $a = 8.75(3)$ Å, $b = 7.16(4)$ Å, $c = 6.88(3)$ Å, $\alpha = 99.05(5)^\circ$, $\beta = 109.35(6)^\circ$, $\gamma = 82.33(7)^\circ$ ($Z = 1$). The Cu^{2+} ion in the unit cell is surrounded by a distorted octahedron of six oxygen atoms, four of which belong to formate ions and the other two to water molecules. The barium ion also has a more or less octahedral coordination from six oxygen atoms ($4HCOO^-$ and $2H_2O$). Three crystallographically inequivalent formates groups exist in the crystal lattice. The water molecules also fall in two sets—$H_2O(1)$ and $H_2O(2)$—which show differences in the Me–O bond lengths. $H_2O(1)$ molecules are bonded to copper atoms and $H_2O(2)$ to barium atoms.

The copper, nickel and zinc double salts have been obtained in the corresponding ternary salt–salt–water systems at 25 °C [5–7]. It was of interest to establish the ability of the Fe^{2+} ions to form a double salt of the formula type $Ba_2Me(HCOO)_6{\cdot}4H_2O$.

The purpose of this paper was to study the solubility diagram of the $Ba(HCOO)_2$–$Fe(HCOO)_2$–H_2O system at 25 °C and characterize the new phases obtained by X-ray powder diffraction and thermal analysis. There are no literature data on the cocrystallization of barium and iron(II) formates.

---

* Fax: +359-2-70-50-24.
E-mail address: vzvass@svr.igic.bas.bg (V.Z. Vassileva).

0040-6031/02/$ – see front matter © 2002 Elsevier Science B.V. All rights reserved.
PII: S0040-6031(02)00398-2

2. Experimental

The formates of barium and iron(II) were prepared by neutralization of dilute formic acid (1:1) with iron powder and barium carbonate, respectively, at 70–80 °C. The metal formate solutions were filtered and concentrated. Crystals were obtained after cooling the solutions to room temperature, then recrystallized from distilled water and dried in air. The crystallization of iron(II) formates occurs in the presence of formic acid to prevent Fe^{2+} oxidation. Chemical and X-ray powder analysis showed that $Ba(HCOO)_2$ [8] and $Fe(HCOO)_2{\cdot}2H_2O$ [9] were obtained. The other reagents used were of analytical grade.

The solubility in the $Ba(HCOO)_2$–$Fe(HCOO)_2$–H_2O system was studied by the Khlopin method [10] of isothermal decrease of supersaturation: aqueous solutions of both the salts, taken in different ratios, were prepared at 60–70 °C, then were cooled in a thermostat at 25 °C and stirred until a constant concentration of the saturated solution, i.e. equilibrium, was achieved. Preliminary experiments showed that the equilibrium in the system was attained in about 15–20 h. The suspension was then filtered and the liquid and the wet solid phases were analyzed. The solubility in the system was determined in the presence of a excess of formic acid (about 4 wt.%) to prevent the Fe^{2+} oxidation. The concentration of the metal ions in both the phases was determined complexometrically as follows: Fe^{2+} at pH 1.5 using sulfosalicylic acid as indicator, after preliminary oxidation of Fe^{2+} to Fe^{3+} with hydrogen peroxide, the sum $Ba^{2+} - Fe^{2+}$ at pH 10 using Eriochrome Black T as indicator, and the Ba^{2+} concentration was calculated by difference. The solid phase composition was determined by graphic method of Schreinemakers for wet residues [11].

X-ray diffraction analysis was carried out with a DRON-3 powder diffractometer using Cu Kα radiation with nickel filter at a scanning speed of 1° min^{-1} in a 2θ diffraction interval of 10–60°. The lattice constants were calculated from diffractometric data by least-squares refinements on the basis of 44 reflections. Thermal investigations were performed on a Paulik-Paulik Erday MOM OD-102 derivatograph. DTA and TG curves were obtained in a static air atmosphere with sample mass of 300 mg, with a heating rate of 10 °C min^{-1} from room temperature to 500 °C using a standard corundum crucible. The reference substance was pure α-Al_2O_3. The DSC measurements were recorded on a Perkin-Elmer DSC-4 instrument up to 400 °C in a dynamic nitrogen atmosphere using standard aluminum pans with heating rates of 10, 2.5 and 1 °C min^{-1} The temperature and sensitivity were calibrated using indium (purity 99.9%) as standard substance.

3. Results and discussion

3.1. Solubility diagram

The solubility data for the $Ba(HCOO)_2$–$Fe(HCOO)_2$–H_2O system at 25 °C are listed in Table 1, and the solubility diagram is shown in Fig. 1. Two crystallization fields are seen in the solubility diagram: a wide crystallization field of $Fe(HCOO)_2{\cdot}2H_2O$ and a comparatively wide crystallization field of a new double salt $Ba_2Fe(HCOO)_6{\cdot}4H_2O$. The crystallization field of $Ba(HCOO)_2$ is very narrow and is limited by the eutonic solution and pure $Ba(HCOO)_2$. It can be seen from the data in Table 1 that a very small amount of Fe^{2+} ions results from the formation of the double salt. The same experimental results were obtained in Refs. [5–7]. The double salt crystallizes from solutions containing 14.54 wt.% $Ba(HCOO)_2$ and 1.26 wt.% $Fe(HCOO)_2$ up to solutions containing 22.47 wt.% $Ba(HCOO)_2$ and 0.15 wt.% $Fe(HCOO)_2$.

The double salt has been isolated from the system by filtering, washing with alcohol and drying in air, and then identified by chemical analysis, X-ray powder diffraction, differential thermal analysis (DTA) and calorimetric analysis (DSC).

$Ba_2Fe(HCOO)_6{\cdot}4H_2O$ forms colorless crystals. The chemical analysis shows 60.35 wt.% $Ba(HCOO)_2$ and 15.26 wt.% $Fe(HCOO)_2$ (theoretical composition: 60.75 and 15.87 wt.%, respectively). There is no indication about the double salt in the literature.

3.2. X-ray diffraction data

X-ray powder diffraction phase analysis confirms the results of the solubility diagram data, indicating the formation of a new solid phase in the system. The diffraction pattern of $Ba_2Fe(HCOO)_6{\cdot}4H_2O$ is similar to that of $Ba_2Me(HCOO)_6{\cdot}4H_2O$ (Me = Co, Ni, Cu, and Zn) [3–7], showing that the five double

Table 1
Solubility in $Ba(HCOO)_2$–$Fe(HCOO)_2$–H_2O system at 25 °C

Liquid phase (wt.%)		Wet solid phase (wt.%)		Solid phase
$Ba(HCOO)_2$	$Fe(HCOO)_2$	$Ba(HCOO)_2$	$Fe(HCOO)_2$	
23.35	–	–	–	$Ba(HCOO)_2$
23.14	0.25	65.91	5.11	Eutonics
22.09	0.27	52.79	15.58	$Ba_2Fe(HCOO)_6{\cdot}4H_2O$
20.15	0.31	55.89	16.27	$Ba_2Fe(HCOO)_6{\cdot}4H_2O$
18.80	0.35	53.93	15.15	$Ba_2Fe(HCOO)_6{\cdot}4H_2O$
17.76	0.47	52.41	14.97	$Ba_2Fe(HCOO)_6{\cdot}4H_2O$
16.05	0.76	54.08	16.11	$Ba_2Fe(HCOO)_6{\cdot}4H_2O$
14.89	1.07	51.17	15.03	$Ba_2Fe(HCOO)_6{\cdot}4H_2O$
14.59	1.29	32.57	40.21	Eutonics
14.40	1.26	4.61	54.76	$Fe(HCOO)_2{\cdot}2H_2O$
12.10	1.19	4.23	51.13	$Fe(HCOO)_2{\cdot}2H_2O$
8.34	1.31	2.27	58.08	$Fe(HCOO)_2{\cdot}2H_2O$
4.15	2.00	1.32	55.49	$Fe(HCOO)_2{\cdot}2H_2O$
–	4.20	–	–	$Fe(HCOO)_2{\cdot}2H_2O$

salts are isostructural. The existence of an iron(II) double salt of the same type is probably connected with the size of the ionic radii of Fe^{2+} (0.78 Å) which is close to those of cobalt (0.75 Å), nickel (0.69 Å), copper (0.73 Å) and zinc (0.74 Å). However, in the $Ba(HCOO)_2$–$Mn(HCOO)_2$–H_2O system at 25 °C a double salt is not found [12]. The ionic radii of Mn^{2+} is 0.83 Å and probably is too large to realize a stable

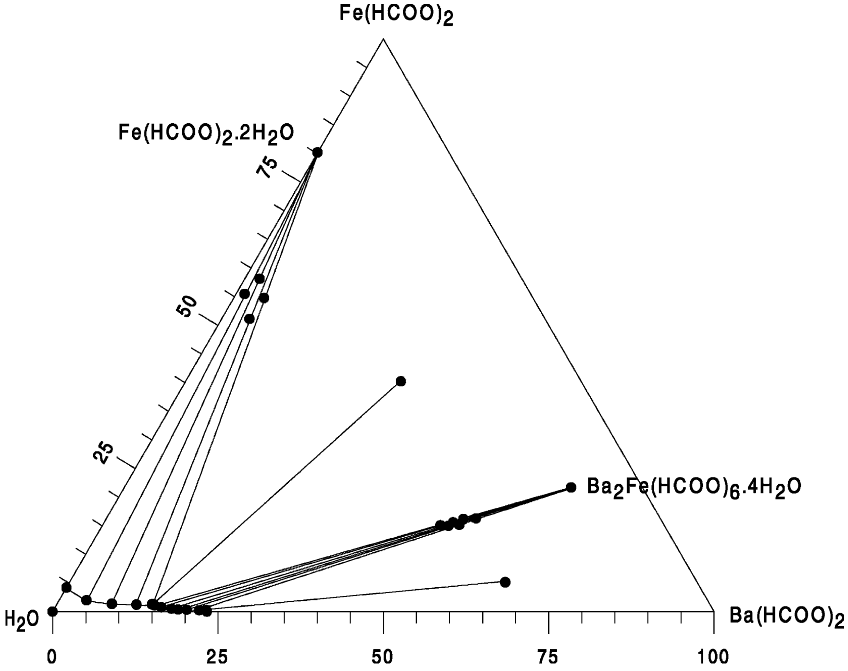

Fig. 1. Solubility diagram of the $Ba(HCOO)_2$–$Fe(HCOO)_2$–H_2O system at 25 °C (in mass%).

crystal structure of the type above. The iron(II) analogue crystallizes also in the triclinic system (space group P$\bar{1}$) with lattice parameters: $a = 8.902(3)$ Å, $b = 7.125(2)$ Å, $c = 6.901(3)$ Å, $\alpha = 98.85(5)^\circ$, $\beta = 108.81(4)^\circ$, $\gamma = 82.47(3)^\circ$, and $V = 407.84$ Å^3(3). The d-spacings, $h\,k\,l$ indices and relative intensities of the 44 reflections are given in Table 2.

3.3. Thermal behavior of $Ba_2Fe(HCOO)_6{\cdot}4H_2O$

The thermal dehydration and decomposition of $Ba_2Fe(HCOO)_6{\cdot}4H_2O$ have been studied by TG, DTA and DSC.

Table 3 presents the data of the thermal dehydration and decomposition of the double salt from DTA and TG analysis. The results coincide with those of the isostructural nickel, zinc and copper analogues, reported in [5–7]. Under our experimental conditions at a heating rate of 10° min^{-1} the dehydration begins at about 120 °C and ends at about 230 °C. The dehydration is registered on the DTA curve with a strong endothermic effect with the maximum at 150 °C and occurs in one step. The mass loss, calculated from the TG curve, corresponds to the loss of four water molecules. According to the structural data of the isostructural double salts $Ba_2Me(HCOO)_6{\cdot}4H_2O$ there are two types of water molecules and is expected that the dehydration proceeds in two steps. But the difference between the Me–O bond lengths in two types of water molecules is small and does not lead to the resolution of the two dehydration steps. As a result of the dehydration an anhydrous product $Ba_2Fe(HCOO)_6$ is formed which is stable in the temperature interval (180–270 °C). A small exothermic effect on the DTA curve at 220 °C is probably due to the crystallization of the amorphous anhydrous salt (there are no mass loss on the TG curve). The decomposition of the double salt begins at about 270 °C and ends at about 400 °C. The two processes, the decomposition of the double salt and the decomposition of $Ba(HCOO)_2$ and $Fe(HCOO)_2$, occur simultaneously. For this reason the thermal decomposition of $Ba_2Fe(HCOO)_6$ is complicated and produces three exothermic effects with maximums at 320, 350 and 380 °C, respectively (see Table 3). The result of the X-ray analysis show that the final decomposition products at about 500 °C are $BaCO_3$ [13] and α-Fe_2O_3 [14] which is in agreement with the literature data [15–18].

Table 2
X-ray diffraction data of $Ba_2Fe(HCOO)_6{\cdot}4H_2O$

$h\,k\,l$	d_{obs} (Å)	I/I_0
1 0 0	8.39	43
0 1 0	7.01	10
0 0 1	6.49	100
1 0 −1	6.13	20
1 1 0	5.63	87
0 1 −1	5.07	40
2 0 0	4.20	10
2 0 −1	4.15	23
2 1 0	3.76	21
1 1 1	3.72	24
0 2 0	3.50	36
−2 1 0	3.47	65
1 0 −2	3.39	18
−2 1 1	3.35	10
1 2 0	3.33	28
1 1 −2	3.27	4
0 0 2	3.24	6
−1 2 0	3.13	24
2 0 1	3.11	12
3 0 −1	2.918	20
2 1 1	2.853	56
0 1 2	2.819	31
−1 2 1	2.816	31
1 0 2	2.753	25
1 2 1	2.720	5
3 1 0	2.681	22
−2 1 2	2.643	4
−2 2 0	2.583	7
−3 1 1	2.566	32
3 1 −2	2.534	15
1 1 2	2.502	6
2 2 1	2.335	30
1 3 0	2.303	7
−1 2 2	2.266	18
3 2 −2	2.249	22
−4 0 1	2.206	21
−3 1 −1	2.185	6
−2 2 2	2.129	5
0 3 1	2.120	12
−3 2 0	2.101	10
−1 3 1	2.067	14
3 1 −3	2.063	14
0 2 −3	1.946	14
2 2 2	1.865	15

The DSC curve of $Ba_2Fe(HCOO)_6{\cdot}4H_2O$ at a heating rate of 10° min^{-1} from 40 to 400 °C, presented in Fig. 2, shows an analogy with the DTA data. A strong endothermic effect at $T_{onset} = 122.54$ °C ($T_{max} = 133.51$ °C) corresponds to the loss of four

Table 3
Data for the thermal decomposition of $Ba_2Fe(HCOO)_6{\cdot}4H_2O$

Transformation	$\Delta m/m$ (%)		T_{max} (°C), DTA
	Observed	Calculated	
$Ba_2Fe(HCOO)_6{\cdot}4H_2O \rightarrow Ba_2Fe(HCOO)_6$	10.81	10.73	150
Amorphous phase → crystalline phase	0	0	220
$Ba_2Fe(HCOO)_6 \rightarrow BaCO_3 + \alpha\text{-}Fe_2O_3$	18.83	18.33	320, 350, 380

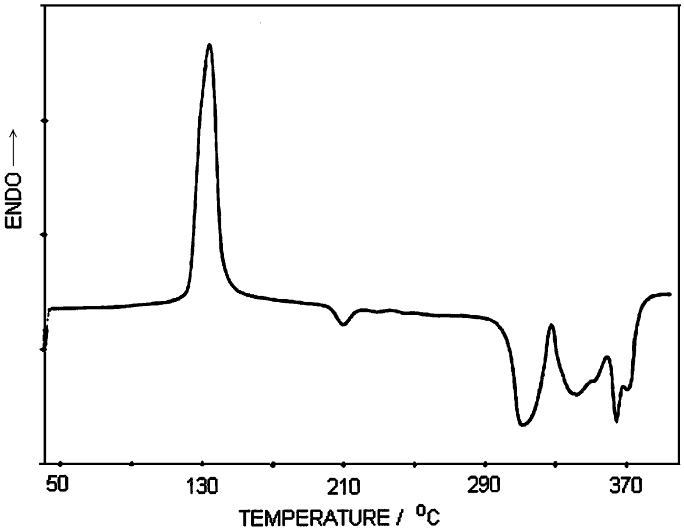

Fig. 2. DSC curve of $Ba_2Fe(HCOO)_6{\cdot}4H_2O$ at 10 °C min^{-1}.

water molecules, thus forming $Ba_2Fe(HCOO)_6$. The dehydration occurs in one step at this heating rate. The enthalpy of dehydration of $Ba_2Fe(HCOO)_6{\cdot}4H_2O$ has been calculated, $\Delta_{deh}H = 200.87\,kJ\,mol^{-1}$. The anhydrous product is stable in the temperature interval of 170–285 °C. A small exothermic peak is observed at 201.97 °C (due to the crystallization of amorphous phase). The peaks at 311.19, 339.35 and 364.4 °C on the DSC curve (exothermic effects) correspond to the decomposition processes of the anhydrous double salt.

The dehydration of $Ba_2Fe(HCOO)_6{\cdot}4H_2O$ was studied by DSC method at a lower heating rate. In Fig. 3(a) and (b) the DSC curves are shown at 2.5 and 1 °C min^{-1}, respectively, in the temperature range of 40–250 °C. It is seen from the figure, that at these heating rates the endothermic effect is splitted, with T_{max} = 123.12 °C and T_{max} = 128.07 °C at 2.5 °C min^{-1} and T_{max} = 121.0 °C and T_{max} =

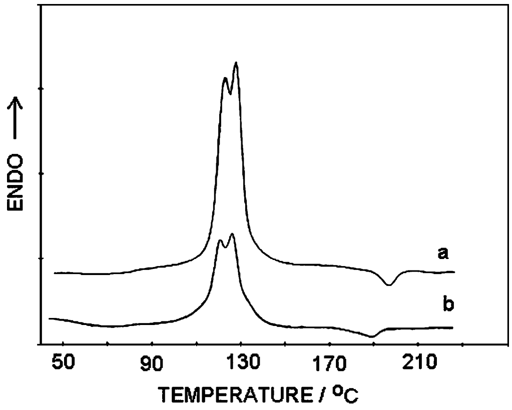

Fig. 3. DSC curves of $Ba_2Fe(HCOO)_6{\cdot}4H_2O$ at (a) 2.5 and (b) 1 °C min^{-1}.

126.08 °C at 1 °C min^{-1}. By analogy with the structural data of $Ba_2Cu(HCOO)_6{\cdot}4H_2O$ [3] and its infrared spectrum [4] this split is due to a two-stage separation of the four water molecules. The $H_2O(2)$ molecules which are bonded to barium ions form longer bonds than the $H_2O(1)$, bonded to copper ions [3]. Therefore the $H_2O(2)$ molecules expected to separate at lower temperature than the $H_2O(1)$ molecules.

4. Conclusion

The solubility diagram of $Ba(HCOO)_2$–$Fe(HCOO)_2$–H_2O system has been investigated at 25 °C showing the formation of a new double salt $Ba_2Fe(HCOO)_6{\cdot}4H_2O$.X-ray powder diffraction analysis shows that the dibarium iron(II) formate tetrahydrate is isostructural with the double salts of the type $Ba_2Me(HCOO)_6{\cdot}4H_2O$ (Me = Co, Ni, Cu, and Zn). The existence of the iron(II) analogue of the same crystal structure is associated with the similar size of the ionic radii of Fe^{2+}. No double salt is formed in the system with mangan(II) formate which indicates that this crystal structure is stable when the ionic radii of Me^{2+} is below 0.83 Å.

The DTA and TG data of $Ba_2Fe(HCOO)_6{\cdot}4H_2O$ were in agreement with those of the isostructural double salts of copper, nickel and zinc. The dehydration leads to an anhydrous $Ba_2Fe(HCOO)_6$. The final decomposition products are $BaCO_3$ and α-Fe_2O_3. The DSC study at lower heating rates indicates a two step of dehydration, which is in accordance with the existence of two crystallographical inequivalent water molecules in the crystal structure. From the DSC data the enthalpy of dehydration has been calculated.

References

[1] W. Lossen, G. Voss, Liebigs Ann. 266 (1891) 15.
[2] P. Groth, Chem. Krist. 3 (1910) 11.
[3] R.V.G. Sundara Rao, K. Sundaramma, G. Sivasankara Rao, Z. Kristallogr. 110 (1958) 231.
[4] D. Stoilova, V. Koleva, Cryst. Res. Technol. 32 (1997) 865.
[5] S.M. Portnova, Y.I. Krasilov, N.T. Kuznetsov, I.V. Balakaeva, Zh. Neorgan. Khim. 35 (1990) 237.
[6] A.A. Fakeev, N.N. Samophalova, L.D. Ishakova, B.V. Zhadanov, Zh. Prikl. Khim. 72 (1999) 1262.
[7] A.A. Fakeev, N.N. Samophalova, L.D. Ishakova, B.V. Zhadanov, Zh. Prikl. Khim. 73 (2000) 180.
[8] JSPDS, Powder Diffraction File, vol. 39, Card 0701.
[9] JSPDS, Powder Diffraction File, vol. 19, Card 0604.
[10] V.G. Khlopin, Izbrannye Trudy (Selected Works), vol. 1, Izd. Acad. Nauk SSSR, Moscow, 1957, p. 162.
[11] F.A.H. Schreinemakers, Z. Phys. Chem. 11 (1893) 76; F.A.H. Schreinemakers, Z. Phys. Chem. 55 (1906) 71.
[12] A.A. Fakeev, L.D. Ishakova, N.N. Samophalova, Zh. Prikl. Khim. 73 (2000) 532.
[13] JSPDS, Powder Diffraction File, vol. 45, Card 1471.
[14] JSPDS, Powder Diffraction File, vol. 13, Card 0534.
[15] D.K. De, S.K. Chawla, A.K. Pal, J. Phys. Chem. Solids 43 (1982) 1017.
[16] G. Liptay, Atlas of Thermoanalytical Curves, vol. 1, N 33, Akademiai Kiado, Budapest, 1977.
[17] D. Vega, G. Polla, A.G. Leyva, H. Lanza, P.K. de Perazzo, R. Baggio, M.A.R. de Benyacar, J. Ellena, H. Tolentino, M. do Carmo Martins Alves, J. Solid State Chem. 147 (1999) 545.
[18] P. Baraldi, Spectrochim. Acta A 35 (1979) 1003.